https://doi.org/10.31436/iiumej.v26i3.3825

NUMERICAL INVESTIGATION OF SEDIMENT SCOUR DOWNSTREAM OF ADJUSTABLE AND FIXED SUBMERGED WEIR USING FLOW-3D

SITI NURAIN CHE MOHD AZMI, SAERAHANY LEGORI IBRAHIM*, IZIHAN IBRAHIM, DANI IRWAN MASBAH

Civil Engineering Department, Kulliyah of Engineering, International Islamic University Malaysia, Kuala Lumpur, Malaysia

**Corresponding author: saerahany@iium.edu.my*

(Received: 2 July 20205; Accepted: 27 July 2025; Published online: 9 September 2025)

ABSTRACT: Scouring downstream of hydraulic structures poses significant risks to structural stability and sediment transport processes in river systems. This study presents a numerical investigation of sediment scour behaviour downstream of two submerged weir types, adjustable submerged weirs (hydraulic tilting gates) and fixed submerged weirs (Crump weirs), using FLOW-3D software. Field measurements from Acoustic Doppler Current Profiler (ADCP) surveys were used to validate the hydrodynamic model, with a finer mesh size of 1.5 m achieving high accuracy (R^2 = 0.998, RMSE = 0.018 m). This mesh size was subsequently adopted for sediment transport simulations. The research focuses on evaluating velocity at the bed and scour depth under a range of flow discharge series, from 183.30 m^3/s to 3666.00 m^3/s, over a 2-year ARI for the Kelantan River, across 20 simulation runs, with low, moderate, and high discharges, classified using a percentile-based approach. The simulations adopt the Reynolds-Averaged Navier-Stokes (RANS) equations with the RNG turbulence model, coupled with the Meyer-Peter and Müller sediment transport formulation. Results reveal that the adjustable submerged weir generally produces higher bed-level velocities at low to moderate discharges, indicating a tendency toward more concentrated local scour. This is likely due to the flow being constricted and accelerated as it passes over and through the adjustable structure, thereby increasing shear stress on the bed. In contrast, the fixed Crump weir exhibits significantly higher peak velocities under extreme flow conditions, leading to broader but less focused erosion patterns, likely because its fixed geometry causes the flow to spread out more evenly downstream, reducing localised acceleration but increasing the overall area affected by erosion. Scour depth analysis reveals that the adjustable weir induces deeper scour holes, with a maximum depth of -5.917 m, whereas the fixed weir reaches a maximum depth of -4.128 m. These outcomes highlight the influence of structural geometry and operational flexibility on downstream hydraulic behaviour and sediment response.

ABSTRAK: Hakisan di hilir struktur hidraulik boleh menjejaskan kestabilan struktur dan proses pengurusan sedimen sungai. Kajian ini menjalankan analisis berangka terhadap keadaan hakisan sedimen pada dua jenis empangan tenggelam iaitu empangan tenggelam boleh laras (pintu hidraulik condong) dan empangan tenggelam kekal (empangan Crump), menggunakan perisian FLOW-3D. Pengukuran lapangan menggunakan Doppler Akustik Pembukah Semasa (ADCP) digunakan bagi mengesahkan model hidrodinamik, di mana saiz mesh lebih halus 1.5 m mencapai ketepatan tinggi (R^2 = 0.998, RMSE = 0.018 m). Seterusnya digunakan bagi simulasi pengangkutan sedimen. Kajian ini memfokuskan pada penilaian halaju pada dasar sungai dan kedalaman hakisan bagi beberapa siri pelepasan aliran sungai berkelajuan antara 183.30 m^3/s hingga 3666.00 m^3/s selama tempoh 2 tahun (ARI) di Sungai Kelantan. Ia melibatkan 20 siri simulasi, dengan aliran rendah, sederhana dan tinggi yang

diklasifikasikan menggunakan pendekatan berasaskan persentil. Simulasi ini menggunakan persamaan Navier-Stokes Purata-Reynolds (RANS) dengan model pergolakan RNG, digabungkan bersama rumusan Meyer-Peter dan Müller bagi pengangkutan sedimen. Dapatan kajian menunjukkan empangan tenggelam boleh laras menghasilkan halaju dasar lebih tinggi pada aliran rendah hingga sederhana, mendorong kepada hakisan setempat yang bertumpu. Hal ini berkemungkinan disebabkan oleh aliran yang tersekat dan dipercepatkan ketika melalui struktur boleh laras, lalu meningkatkan tegasan ricih pada dasar sungai. Sebaliknya, empangan Crump jenis kekal menunjukkan halaju puncak lebih tinggi semasa aliran deras, menghasilkan corak hakisan yang lebih meluas tetapi kurang bertumpu, kerana geometri kekal menyebabkan aliran tersebar lebih sekata di hilir, sekaligus mengurangkan pecutan setempat, tetapi memperluas kawasan yang terjejas oleh hakisan. Analisis kedalaman hakisan mendedahkan bahawa empangan boleh laras menghasilkan lubang hakisan yang lebih dalam, dengan kedalaman maksimum -5.917 m, manakala empangan kekal mencapai kedalaman maksimum -4.128 m. Dapatan ini menekankan pengaruh geometri struktur dan fleksibiliti operasi pada keadaan hidraulik hilir serta respon sedimen.

KEY WORDS: *Scouring, Submerged Weir, Hydraulic Tilting Gate, Crump Weir, FLOW-3D*

1. INTRODUCTION

1.1. Scouring

Scouring refers to the erosion process caused by flowing water that removes sediment from the riverbed [1], often leading to significant changes in bed morphology downstream of hydraulic structures such as submerged weirs. This phenomenon is critical because excessive scour can compromise the stability and safety of these structures, potentially resulting in structural failure and associated economic losses [2]. Numerous studies have investigated scour downstream of submerged weirs, focusing on various factors influencing scour depth and geometry, including flow conditions, sediment characteristics, and weir design.

Previous research has demonstrated that the shape and height of weirs significantly affect the development of scour holes. For example, experimental studies comparing different weir geometries have shown that rectangular weirs tend to produce 36-56% deeper scour holes compared to trapezoidal weirs under similar flow conditions, with near-bed velocities of 2-3 m/s that generate 15 N/m², intensifying the scouring process [3]. Additionally, the flow regime, whether free-flow or submerged, also plays a critical role. Based on Figure 1, submerged weirs under live bed conditions exhibit fluctuating scour depths due to migrating bedforms, with equilibrium depths 10% lower than clear water scour scenarios [4].

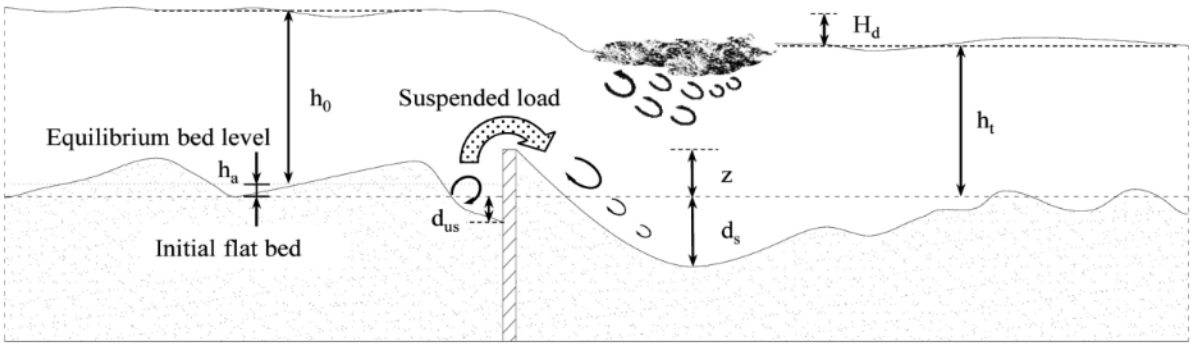

Figure 1. Illustration of a submerged weir's live bed scour [5].

https://doi.org/10.31436/iiumej.v26i3.3825

1.2. Study Area

The Kasa Low Weir in Pasir Mas, Kelantan, was constructed to regulate water levels for the pump stations that support paddy field irrigation. Completed on 19th April 2016 with a crest level of 1.8 m, the structure included adjustable submerged weirs, comprising two hydraulic tilting gates and a navigation lock for regulating water levels and facilitating boat passage. However, on 11th June 2018, two years after completion, a 130-meter section between the gates collapsed due to severe scouring, disrupting water regulation. A forensic investigation by the Department of Irrigation and Drainage (DID) in 2020 revealed extensive scour both upstream and downstream, particularly around the tilting gates, with depths ranging from -2 m to -14 m as depicted in Figure 2. The failure was attributed to the structure's inability to withstand hydrodynamic forces, causing seepage and scour. Due to ongoing instability, a Crump weir design as a fixed weir was one of the proposed designs for the upcoming rehabilitation, offering a more stable discharge coefficient to improve hydraulic performance and reduce the risk of future failure.

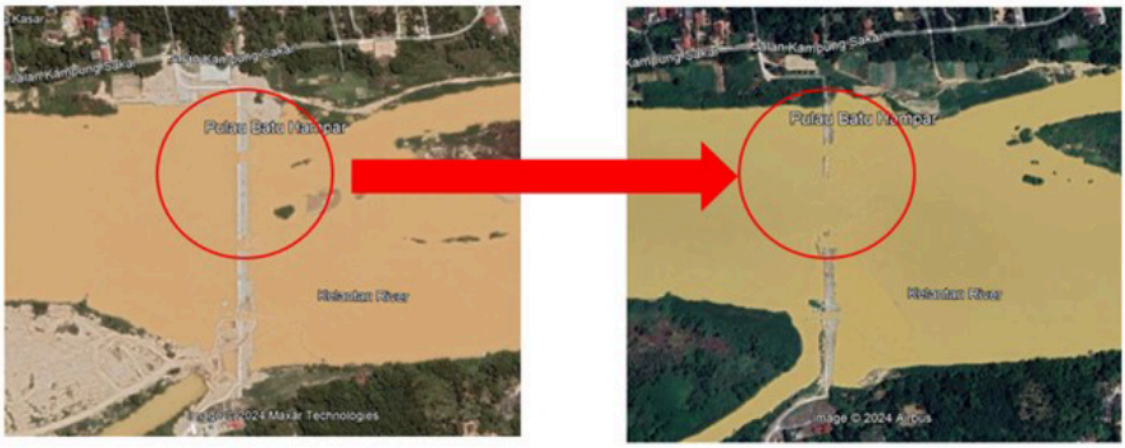

Figure 2. The area of the hydraulic tilting gates of Kasa Low Weir that has collapsed and washed away due to significant scouring.

1.3. Submerged Weir

Submerged weirs, including both adjustable and fixed types, are hydraulic structures installed below the water surface to regulate flow velocities, stabilise riverbeds, and manage water levels in rivers [6]. These weirs operate under two primary flow regimes: free flow, where downstream water levels remain below the crest, and submerged flow, where tailwater elevations exceed the crest, altering discharge characteristics. Scouring, the erosion of sediment around these structures, poses significant risks to their stability, particularly during high-flow events. For instance, live-bed scour conditions, where sediment transport occurs continuously, create dynamic bedforms that amplify scour depths downstream of submerged weirs [7-8].

Adjustable and fixed submerged weirs employ distinct mechanisms to mitigate scouring effects, striking a balance between hydraulic efficiency and structural resilience. While numerous studies have investigated hydraulic behaviour and associated scouring patterns downstream of submerged weirs, most have focused on either adjustable or fixed types in isolation, often through experimental setups with limited discharge scenarios. As a result, there is a lack of comprehensive, side-by-side numerical comparisons under identical flow conditions, particularly using computational fluid dynamics (CFD) modelling such as FLOW-3D [9]. This study presents a numerical comparison of sediment scour downstream of adjustable and fixed submerged weirs, which helps improve the understanding of both weir

https://doi.org/10.31436/iiumej.v26i3.3825

design and its influence on scouring, leading to better design and sediment management in rivers.

Submerged weirs are widely used in river engineering to regulate flow and manage sediment transport, but their performance in resisting downstream scouring varies depending on their design. Adjustable submerged weirs, such as hydraulic tilting gates, offer operational flexibility, while fixed weirs like the Crump type provide geometric stability. However, how these design differences influence flow behaviour and scouring under different flow conditions remains insufficiently explored. A direct comparison between the two is necessary better to understand their hydraulic performance and impact on bed erosion.

1.3.1. Adjustable Submerged Weir (Hydraulic Tilting Gate)

Adjustable submerged weirs, such as hydraulic tilting gates, offer operational flexibility to control water discharge and maintain desired upstream levels. The structural systems alter crest heights (± 2 mm precision) to optimise discharge distribution, reducing shear stresses during high-flow events [10-11]. These systems utilize rotational mechanisms around a horizontal axis to modulate discharge capacity, allowing for real-time adaptation to fluctuating hydrological conditions, such as flood events or sediment-laden flows. However, this adjustability can lead to varying flow regimes, which in turn influence the development and extent of cyclical scour patterns downstream. Past studies reveal that adjustable weirs under live-bed conditions experience oscillating scour depths (up to 44% variation) due to alternating jet intrusion and deposition phases [12]. Experimental analyses using particle image velocimetry (PIV) reveal that turbulence intensities near tilting gates reach 2.5 times the upstream values, creating sediment entrainment pulses synchronised with the gate opening [13]. The dynamic nature of flow over these gates often results in complex turbulence and sediment transport processes, necessitating detailed analysis to predict scour characteristics downstream of the structure.

1.3.2. Fixed Submerged Weir (Crump Weir)

Fixed submerged weirs, such as the Crump weir, rely on geometric stability to induce predictable scour patterns. This structure, characterised by triangular profiles with upstream slopes of 1:2 and downstream slopes of 1:5, maintains predictable performance under modular flow [14]. Under modular flow conditions, Crump weir design maintains a discharge coefficient (Cd) of less than 5% across a 10:1 head range, ensuring reliable performance in a sediment-laden environment [15]. The weir's sloped faces create a cascading energy dissipation mechanism that reduces downstream maximum shear stresses by 54% compared to vertical-faced structures when the tailwater height exceeds 1.2 times the critical depth. The experimental analyses reveals that Crump weirs achieve 23% greater energy dissipation efficiency than tilting gates under equivalent hydraulic loads due to their established crest geometry and optimised slope ratios [16]. The fixed profile of the Crump weir minimises operational complexity and mechanical maintenance, making the Crump weir indispensable for long-term infrastructure resilience against scouring risks.

1.4. FLOW-3D

FLOW-3D employs a finite volume method to solve the three-dimensional, incompressible Reynolds-averaged Navier-Stokes (RANS) equations, coupled with the Volume of Fluid (VOF) technique for tracking free surfaces [17]. The solver integrates the continuity and momentum conservative equations, formulated as Eq. (1) and Eq. (2):

Continuity equation:

https://doi.org/10.31436/iiumej.v26i3.3825

$$\frac{\partial u_i}{\partial x_i} = 0 \tag{1}$$

Momentum equation:

$$\frac{\partial u_i}{\partial \mathrm{t}} + u_j \frac{\partial u_i}{\partial x_j} = -\frac{1}{\rho}\frac{\partial \mathrm{p}}{\partial x_i} + \nu \frac{\partial^2 u_i}{\partial x_j^2} + \frac{\partial \tau_{ij}}{\partial x_j} \tag{2}$$

where τ_{ij} represents Reynolds stresses, which are modelled using turbulence closure schemes. The Fractional Area-Volume Obstacle Representation (FAVOR^{TM}) method is utilised to embed complex geometries into the Cartesian grid, ensuring accurate boundary conditions while minimising mesh generation complexity.

1.4.1. Turbulence Model

The RNG turbulence model was employed for this study for several compelling reasons. First, it is particularly well-suited for simulating turbulent flow over a weir, which is critical for accurately capturing the complex hydrodynamic interactions involved in scour processes. Second, among the turbulence models available in commercial computational fluid dynamics software, the RNG model is recognised for its superior accuracy and robustness in predicting flow behaviour relevant to scouring. Lastly, due to its enhanced capability to account for high levels of turbulence generated by fluid flow through control structures, the RNG model often demonstrates improved performance in scour simulations. The listed attributes collectively justify its selection for the present analysis [18]. The transport equations for turbulent kinetic energy (k) and dissipation rate (ϵ) are according to Eq. (3) and Eq. (4):

$$\frac{\partial(\mathrm{pk})}{\partial \mathrm{t}} + \frac{\partial(\mathrm{pku_j})}{\partial \mathrm{x_j}} = \frac{\partial}{\partial \mathrm{x_j}}\left(\alpha_\mathrm{k}\mu_\mathrm{eff}\frac{\partial \mathrm{k}}{\partial \mathrm{x_j}}\right) + \mathrm{Gk} - \mathrm{p}\epsilon \tag{3}$$

$$\frac{\partial(\mathrm{p}\epsilon)}{\partial \mathrm{t}} + \frac{\partial(\mathrm{p}\epsilon \mathrm{u_j})}{\partial \mathrm{x_j}} = \frac{\partial}{\partial \mathrm{x_j}}\left(\alpha_\mathrm{k}\mu_\mathrm{eff}\frac{\partial \epsilon}{\partial \mathrm{x_j}}\right) + \mathrm{C_{1\epsilon}}\frac{\epsilon}{\mathrm{K}}\mathrm{G_k} - \mathrm{C_{2\epsilon}}\rho\frac{\epsilon^2}{\mathrm{K}} - \mathrm{R}_\epsilon \tag{4}$$

Here, $\mu_{eff} = \mu+\mu_t$, with $\mu_t = \rho C_\mu k^2/\epsilon$. The RNG model introduces the Rϵ term to address rapid strain and streamline curvature effects, enhancing accuracy in flows with high shear or rotation. Unlike the standard k-ε model, the RNG variant dynamically adjusts Cμ (turbulent viscosity coefficient) and employs an analytically derived turbulent Prandtl number (α_k, α_ϵ), reducing reliance on empirical constants.

1.4.2. Sediment Scour Model

The prediction of sediment scouring downstream of weirs is a critical concern in hydraulic engineering, as scouring can undermine the structural stability of these hydraulic control structures. The Meyer-Peter and Müller (MPM) equation is frequently employed within FLOW-3D to simulate bedload sediment transport and scour evolution in such contexts, relating sediment flux to excess shear stress in Eq. (5) [19]:

$$\Phi = 8(\theta - \theta_{\mathrm{cr}})^{1.5} \tag{5}$$

where $\Phi = q_b/\sqrt{g d_{50}^3}$ is the dimensionless bedload transport rate, $\theta = \tau/(\rho g d_{50})$ is the Shields parameter, and θ_{cr} is the critical Shields parameter for incipient motion. The bed shear stress τ is computed from the RNG-resolved velocity field, while θ_{cr} is calibrated using sediment grain size and density [20].

Morphological evolution of the bed is tracked through the Exner equation, as expressed in Eq. (6):

https://doi.org/10.31436/iiumej.v26i3.3825

$$(1 - \lambda_p)\frac{\partial \eta}{\partial t} + \frac{\partial q_b}{\partial x} = 0 \quad (6)$$

where η is bed elevation and λ_p is sediment porosity. FLOW-3D enhances the MPM formulation by incorporating 3-dimensional effects, such as secondary currents and turbulent bursting, which amplify local scour by up to 30% compared to depth-averaged approaches. Scour depth predictions around bridge piers show less than 10% error when validated against experimental data using RNG-resolved turbulence [21].

2. METHODOLOGY

2.1. Model Validation

To assess the depth-averaged velocity along the Kelantan River, Acoustic Doppler Current Profiler (ADCP) instruments were strategically deployed at three key locations: upstream of Sultan Yahya Petra Bridge (Q1/WL1), downstream of Kasa Low Weir (Q2/WL2), and upstream of Sheet Pile Kemumbu structure (Q3/WL3) as presented in Figure 3. Among these, station Q2/WL2, positioned immediately downstream of the Kasa Low Weir, was selected for validation analysis on the FLOW-3D model due to its critical hydrodynamic behaviour influenced by the weir structure. For depth-averaged velocity, data were collected from station Q2, located downstream of Kasa Low Weir, from 13th October 2024 at 17:00 until 2nd November 2024 at 15:40.

Figure 3. Location of ADCP deployed at the Kelantan River.

The validation model was developed based on the actual 1 km upstream and downstream surveyed bathymetry and cross-sectional topography of the Kelantan River at Kasa Low Weir to represent the physical conditions of the study area accurately. In FLOW-3D, the bathymetry was modelled as a fixed bed to focus solely on hydrodynamic analysis, without the influence of sediment transport or bed deformation. This approach allowed for a more precise comparison between the simulated and measured flow characteristics. Validation was performed using field data collected from the ADCP at station Q2/WL2, which is located approximately 1.11 km downstream of the Kasa Low Weir, as shown in Figure 4.

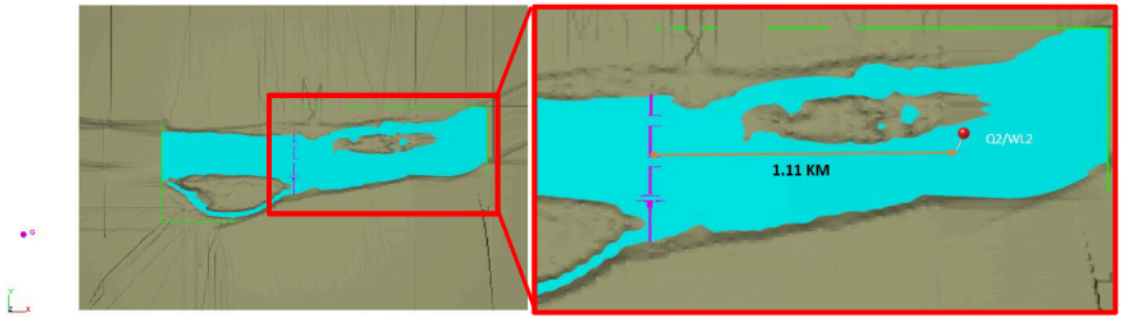

Figure 4. Model setup for validation in FLOW-3D

https://doi.org/10.31436/iiumej.v26i3.3825

To estimate the upstream discharge conditions at the Kasa Low Weir, measurements were carried out using an Acoustic Doppler Current Profiler (ADCP) at Station Q3/WL3, located upstream near the Sheet Pile Kemumbu. On 2 November 2022, depth-averaged velocity and were recorded at 10-minute intervals over one hour from 14:40 to 15:40. During this time, the average current velocity ranged from 0.788 m/s to 0.819 m/s, with an overall average of 0.816 m/s. To ensure accurate discharge calculation, both ADCP probes, Q2 (downstream of the weir) and Q3 (upstream), were deployed in a coordinated way. According to Figure 5, Station Q2 was deployed on 13 October 2022 at 17:50, while Station Q3 was deployed on 15 October 2022 at 11:00. Q2 was retrieved on 2 November 2022 at 15:40, and Q3 on 10 November 2022 at 09:50. Most importantly, both stations collected data at the same time on 2 November 2022 between 14:40 and 15:40. This synchronised measurement ensures consistency when comparing flow conditions upstream and downstream of the weir and improves the accuracy of model validation and discharge estimation.

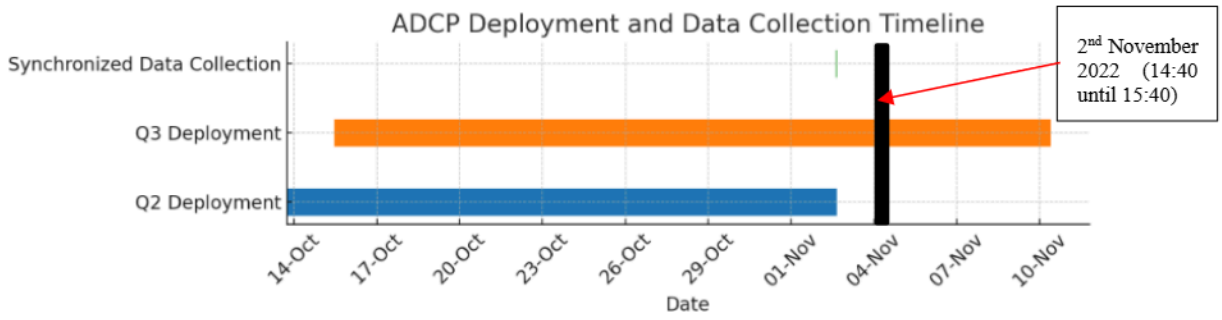

Figure 5. Timeline of ADCP deployments and synchronised data collection.

The upstream discharge was calculated using the area–velocity method. The river cross-section was divided into several segments, each with a measured width of 62.5 m and varying depths from 0.8 m to 6.0 m. This gave a total cross-sectional area of 962.5 m². By multiplying this area by the average velocity of 0.816 m/s, the estimated upstream river discharge was 785.4 m³/s. This value represents typical flow conditions upstream of the Kasa Low Weir and serves as a key input for hydrodynamic validation of the model in Figure 6.

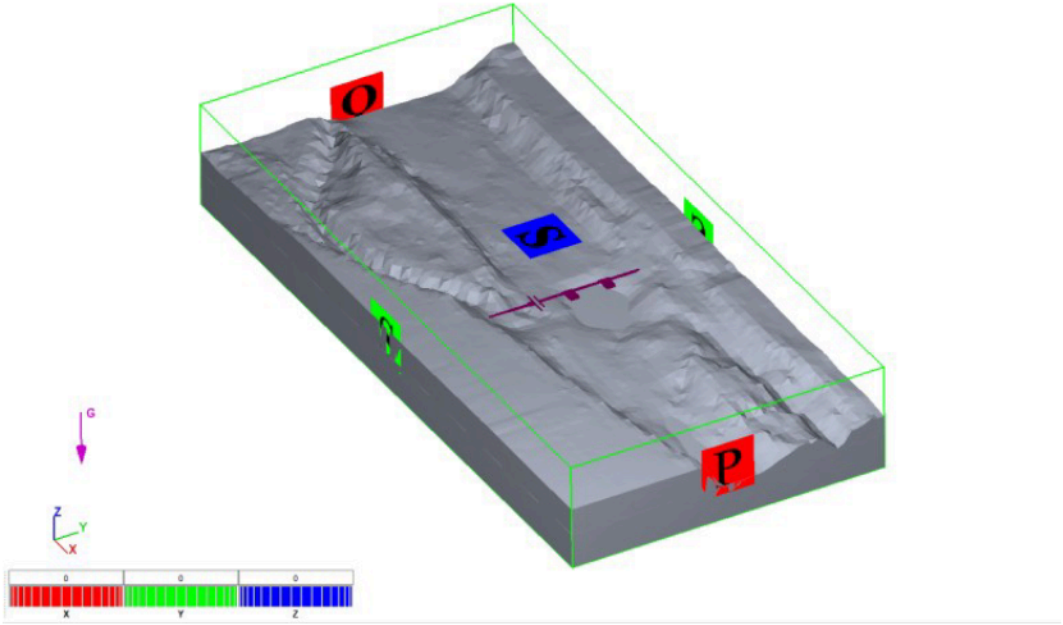

Figure 6. Boundary conditions for model validation.

https://doi.org/10.31436/iiumej.v26i3.3825

The validation of the numerical model will be carried out by comparing the simulated results with observed data obtained from the ADCP. Two different mesh sizes, 1.5 m (finer mesh) and 3.0 m (coarser mesh), will be tested in the model to evaluate the impact of mesh resolution on simulation accuracy, as shown in Figure 7. The comparison will focus on key flow parameters such as depth-averaged velocity at the location of the ADCP probe.

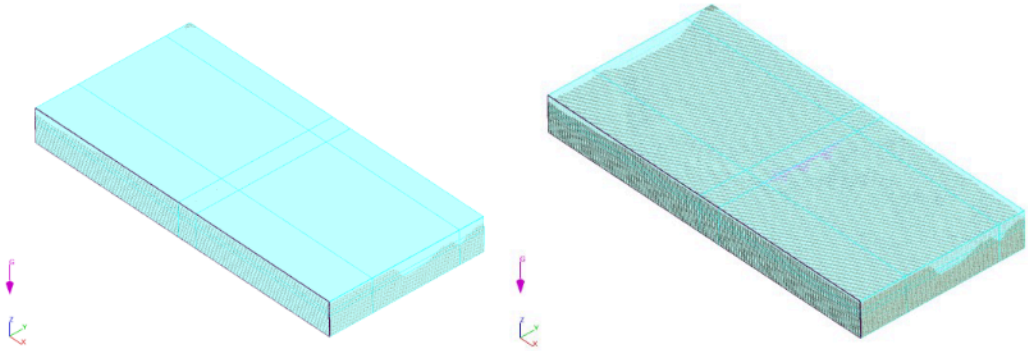

Figure 7. Comparison of validation results using two different mesh sizes (1.5 m and 3.0 m) in the model.

To quantify the agreement between the simulated and observed flow velocity, the mean absolute error (MAE), mean squared error (MSE), and coefficient of determination (R^2) were calculated, as presented in Table 1. The RMSE, MAE, and R^2 are calculated for the data set. Root Mean Squared Error (RMSE) in Eq. (7) serves as a critical measure by quantifying the average magnitude of prediction errors. RMSE computes the square root of the mean squared differences between predicted and observed values, thereby penalising larger deviations more heavily. This characteristic makes RMSE particularly sensitive to significant errors, offering a comprehensive assessment of model accuracy in the same units as the output variable [22].

$$RMSE = \sqrt{\frac{1}{n}\sum_{i=1}^{n}(y_i - \widehat{y_i})^2} \tag{7}$$

In Eq. (8), the Mean Absolute Error (MAE) provides an alternative validation metric that measures the average absolute deviations between predicted and true values without biasing larger errors. By treating all errors uniformly, MAE conveys an interpretable and straightforward metric of model performance, reflecting the expected magnitude of errors in predictions regardless of their direction or scale.

$$MAE = \frac{1}{n}\sum_{i=1}^{n}|y_i - \hat{y}i| \tag{8}$$

The Coefficient of Determination (R^2), as shown in Eq. (9), serves as a statistical index that expresses the proportion of variance in the dependent variable accounted for by the numerical model. R^2 values range from 0 to 1, where higher values indicate stronger explanatory power and a better fit. This metric is essential in validating model effectiveness by quantifying how well the model captures the variability inherent in the observed data, thereby indicating its predictive reliability [23].

$$R^2 = 1 - \frac{\sum_{i=1}^{n}(y_i - \widehat{y_i})^2}{\sum_{i=1}^{n}(y_i - \bar{y})^2} \tag{9}$$

From the equations, the symbol y_i refers to the actual observed value at the i-th data point, which represents the true measurement obtained from field data. $\hat{y}_i$ denotes the predicted value generated by the model at the same i-th point. These two values are compared to assess how closely the model simulates real conditions. The variable n represents the total number of

https://doi.org/10.31436/iiumej.v26i3.3825

observations or data points used in the comparison. Additionally, in the calculation of the coefficient of determination R^2, the mean of all observed values, represented as $\bar{y}$, is used to quantify how much of the variance in the observed data is explained by the model.

Table 1. Comparison of observed and simulated depth-averaged velocity at Station Q2/WL2 for mesh sizes of 1.5 m and 3.0 m over time.

Time step (s)	Observed Data	Simulated Data	
	Station Q2/WL2	1.5 m	3.0 m
0	0.747	0.760	0.740
600	0.754	0.742	0.754
1200	0.772	0.771	0.771
1800	0.681	0.678	0.681
2400	0.719	0.717	0.729
3000	0.135	0.146	0.250
3600	0.101	0.144	0.007

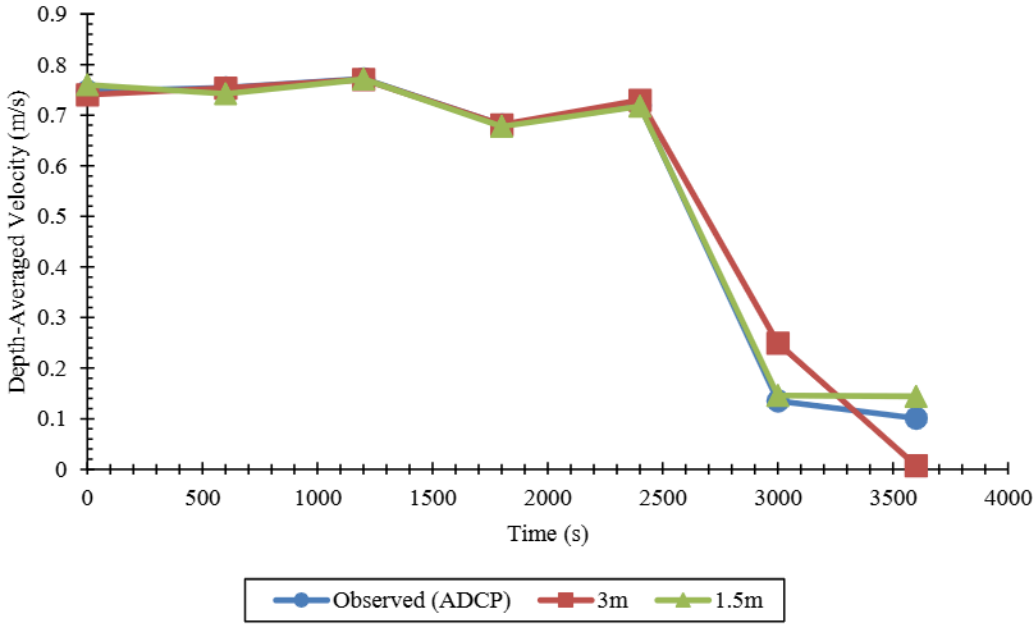

Figure 8. Depth-averaged velocity variation over time from observations and simulations using 1.5 m and 3.0 m mesh sizes.

Table 2: Statistical comparison between simulated and observed flow velocity for different mesh sizes.

Mesh sizes (m)	Root Mean Squared Error (RMSE)	Mean Absolute Error (MAE)	Coefficient of Determination (R^2)
1.5 (finer mesh)	0.018	0.012	0.998
3.0 (coarser mesh)	0.056	0.033	0.961

The comparative analysis between simulated depth-averaged velocity results and the observed ADCP data is presented in both Table 1 and Figure 8. The results show in Table 2 that the finer mesh (1.5 m) closely follows the observed trend across all time steps, with lower error metrics: an RMSE of 0.018 and an MAE of 0.012. In contrast, the coarser mesh (3.0 m) yields a higher RMSE of 0.056 and MAE of 0.033, indicating a greater deviation from the

https://doi.org/10.31436/iiumej.v26i3.3825

observed values. This is further supported by the coefficient of determination (R^2), where the finer mesh achieved 0.998, suggesting a near-perfect fit, while the coarser mesh produced a slightly lower R^2 of 0.961. The performance difference is particularly evident at later steps, at 3000 s until 3600 s, where the 3.0 m mesh significantly underestimates the depth-averaged velocity. Overall, the results demonstrate that finer mesh resolution enhances the model's accuracy in replicating the observed flow behaviour. The results show that the simulated water levels closely match the measured values. While slight deviations were observed at certain points, the overall simulation demonstrates reliable performance. Given its higher accuracy, the 1.5 m mesh size will be selected for the subsequent sediment transport modelling.

2.2. Sediment Transport Model

To focus specifically on sediment transport processes near the structure and to reduce computational time, the full-scale model domain was trimmed to include only the region surrounding the weir. This reduced boundary setup allowed for a more detailed analysis of local scour and sediment dynamics while minimising unnecessary calculations in areas not critical to the study. The refined domain was then imported into FLOW-3D for sediment transport simulation.

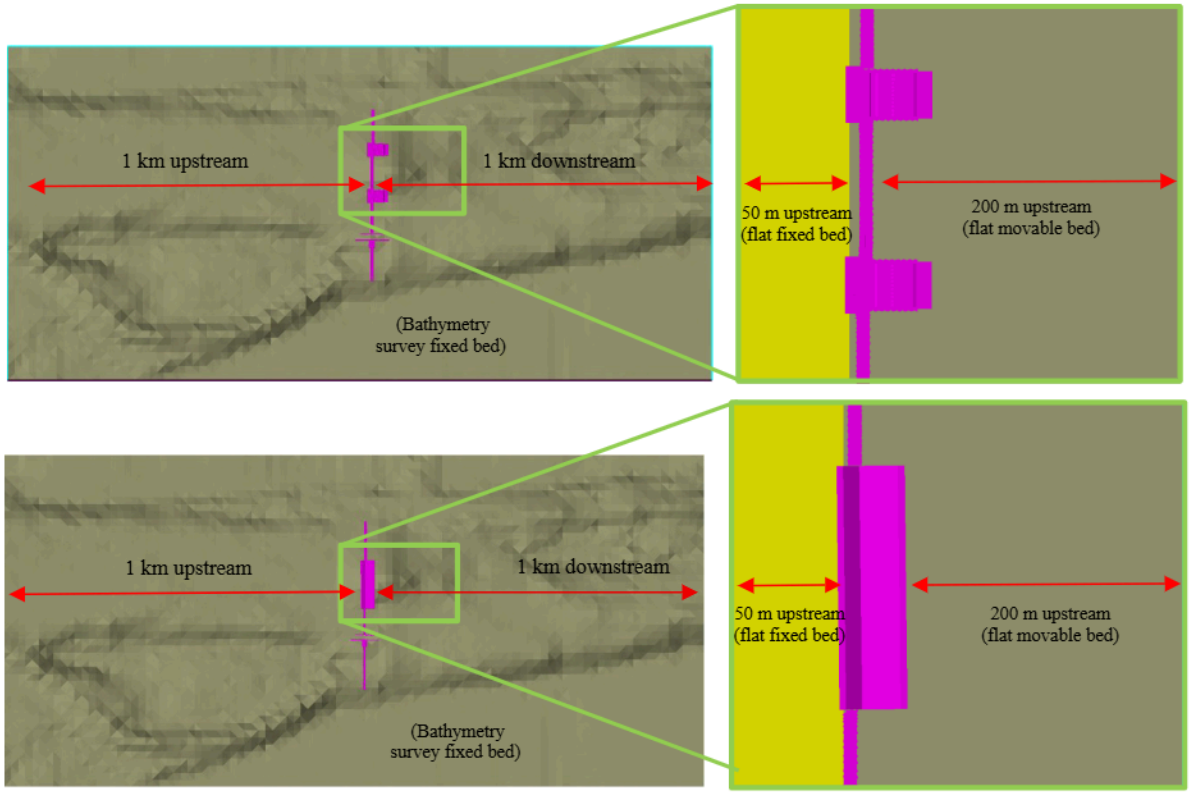

Figure 9. Reduced boundary model around weir structures used for sediment transport simulation.

2.2.1. Geometry Setup

In this study, a comparison is made between an adjustable (two hydraulic tilting gates), which allows active flow control through gate opening for variable flow conditions, and a fixed (Crump weir) submerged weir, a simpler and passive structure that permits overflow based on upstream water levels, as shown in Figure 10(a) and Figure 10(b). In Figure 11(a) and Figure 11(b), the geometry design of the hydraulic tilting gates is based on a real-life project used as

a case study, while the Crump weir is considered as an alternative to replace the gate. Both geometric models are created using SketchUp software.

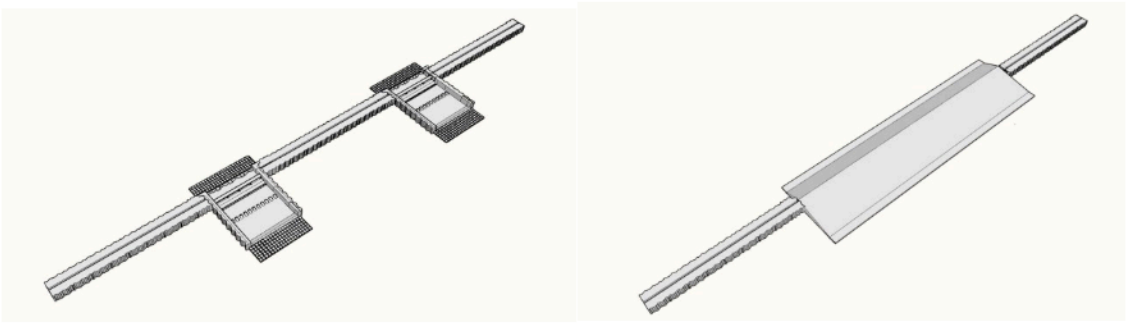

Figure 10. Dimension of (a) hydraulic tilting gate and (b) Crump weir in SketchUp software in isometric view.

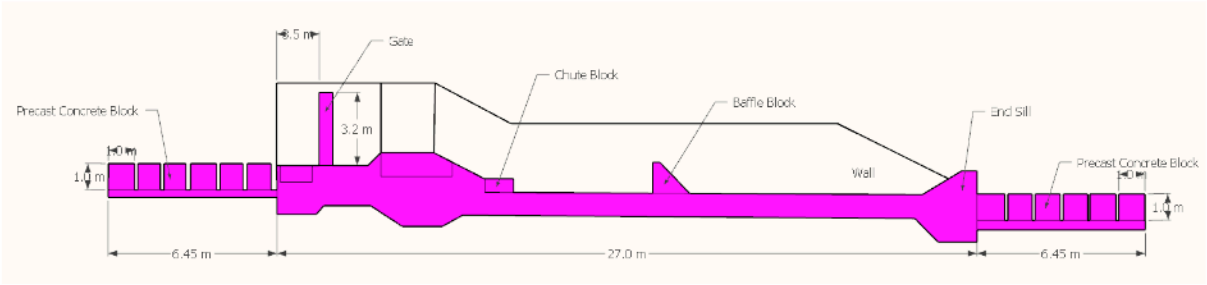

(a)

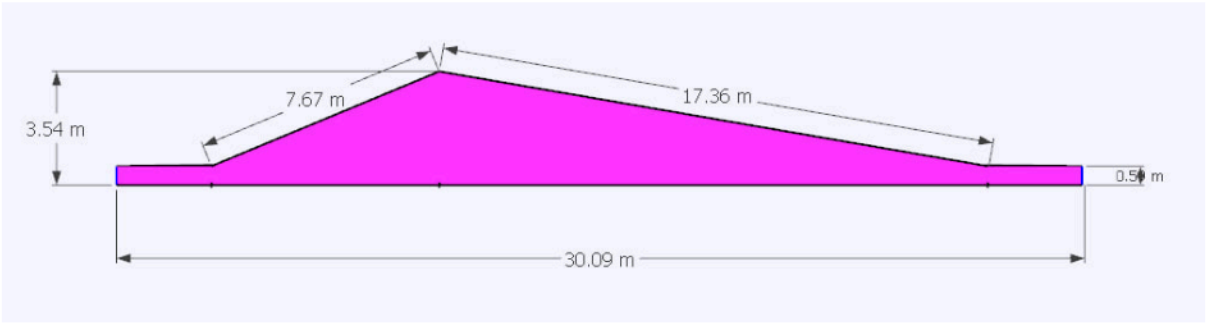

(b)

Figure 11. Dimension of (a) hydraulic tilting gate and (b) Crump weir from side view.

2.2.2. Boundary Setup

In FLOW-3D, specifying the simulation time, physics, fluid characteristics, meshing, boundary conditions, and initial conditions are important parameters for modelling riverbed scouring. The simulation runs for 3600 seconds to accurately capture flow dynamics downstream of both weir structures. The simulation setup includes Shallow Water Approximation, Gravity (Z = -9.81 m/s^2), Turbulence and Viscosity (Renormalised group (RNG) model), and Density (evaluated as a function of other parameters, such as temperature or scalars). To ensure alignment with the actual real-life project water levels, the initial condition sets the fluid elevation at +1.70 m from datum for both weir configurations, as shown in Figure 12(a) and Figure 12(b).

https://doi.org/10.31436/iiumej.v26i3.3825

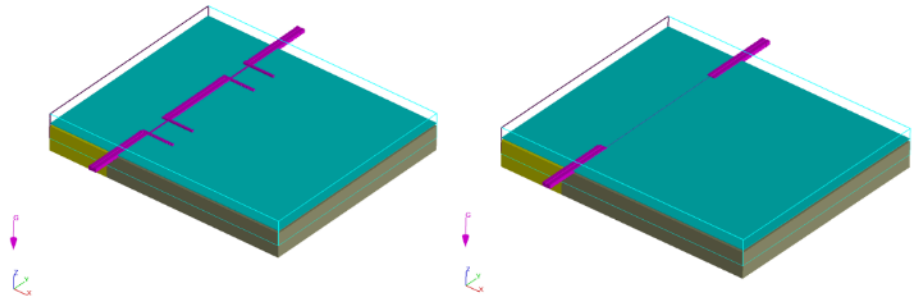

Figure 12. Initial conditions for (a) adjustable submerged weir (hydraulic tilting gate) and (b) fixed submerged weir (Crump weir) model setup configurations.

The summary of the Sediment Transport function for both weir configurations (Meyer-Peter & Müller equation) is as follows, based on the conditions of the Kelantan riverbed as presented in Table 3.

Table 3. Overview of the Sediment Transport Physics in FLOW-3D in this study.

Name	Diameter [m]	Density [kg/m^3]	Critical Shields Number	Entrainment Coefficient	Bed Load Coefficient	Maximum Packing Fraction
Sediment 1	0.0074	2650	0.05	0.018	12	0.0001
Sediment 2	0.0070	2650	0.05	0.018	12	0.0001
Sediment 3	0.0085	2650	0.05	0.018	12	0.0001

Several constraints must be established in FLOW-3D modelling. FLOW-3D imports the geometric model in STL format. As seen in both Figure 13(a) and 13(b), a rectangular flume with 170 m length, 200 m width, and a height of 20 m using the mesh barrier. The dimensions provide enough space for both upstream and downstream hydraulic structures to observe flow behaviour and scour development accurately. The upstream bed was defined as a fixed (solid) bed to maintain stable flow conditions before reaching the weir structure. The downstream bed was modelled as a movable bed, allowing sediment transport and deformation to occur. This configuration was chosen to focus on observing and analysing local scour development downstream of adjustable and fixed submerged weirs under varying flow conditions.

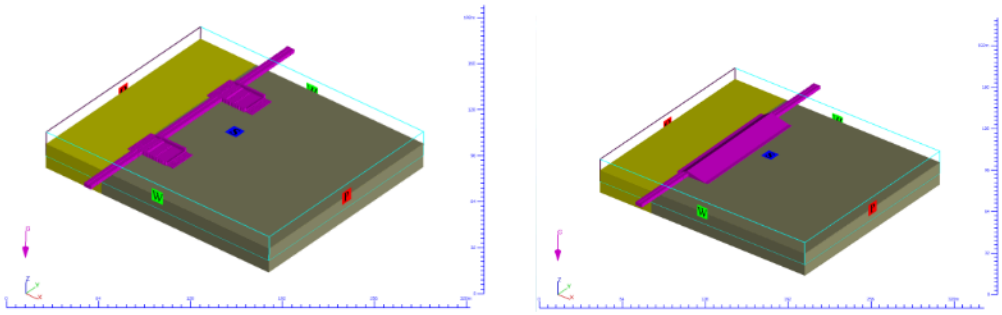

(a) (b)

Figure 13. Boundary setup for both models.

The boundary conditions include Wall (W) for non-slip boundary surfaces, Symmetry (S) to reduce computational load, Specified Pressure at the outlet to control hydrostatic conditions, and Volume Flow Rate (Q) to regulate inflow, representing a range of hydraulic loading conditions. In Table 4, a total of 20 simulations were performed for each structure type, with

https://doi.org/10.31436/iiumej.v26i3.3825

discharge values incrementally increasing from 182.30 m^3/s to 3666.00 m^3/s under a 2-year ARI of the Kelantan River using a percentile-based approach. This range was selected to capture the effects of low to high flow scenarios on the development of local scour downstream of the weirs. The classification into low, moderate, and high discharges is justified using a percentile-based approach [24]. By gradually increasing the flow rate in each simulation, this study was able to observe how different discharge levels affect flow velocity, shear stress, and the pattern of bed erosion around the hydraulic tilting gate and Crump weir.

Table 4: Sediment Transport simulation runs for both the adjustable and fixed submerged weir in this study.

Run(s)	Discharge, Q (m^3/s): Low	Run(s)	Discharge, Q (m^3/s): Moderate	Run(s)	Discharge, Q (m^3/s): High
1	183.30	**8**	1466.40	**15**	2749.50
2	366.60	**9**	1649.70	**16**	2932.80
3	549.90	**10**	1833.00	**17**	3116.10
4	733.20	**11**	2016.30	**18**	3299.40
5	916.50	**12**	2199.60	**19**	3482.70
6	1099.80	**13**	2382.90	**20**	3666.00
7	1283.10	**14**	2566.20		

2.2.3. Meshing Setup

In both Figure 14(a) and Figure 14(b), a structured mesh was generated to ensure accurate and stable numerical simulations in computational fluid dynamics (CFD) analysis [25]. The mesh block was defined as uniform cell sizes of 1.5 meters in the X, Y, and Z directions, resulting in a total of 195,377 cells. The grid was distributed across the domain with 133 cells along the X-axis, 113 cells along the Y-axis, and 13 cells along the Z-axis. To assess mesh quality, key indicators such as the maximum adjacent cell size ratio and maximum aspect ratio were evaluated in Table 5. The maximum adjacent ratios for X, Y, and Z directions were 1.00001, 1.00001, and 1.0000. Similarly, the maximum aspect ratios for each plane (X-Y, Y-Z, and Z-X) were 1.00045, 1.02263, and 1.02308, respectively. To ensure mesh quality, the quantity and spacing of cells in the x, y, and z directions must be configured such that the maximum adjacent cell size ratio remains below 1.25, and the maximum aspect ratio does not exceed 3.0 [26]. These values confirm that the mesh used in the simulation is of high quality, ensuring numerical stability and reliable results for analysing flow and scouring behaviour around the hydraulic structures.

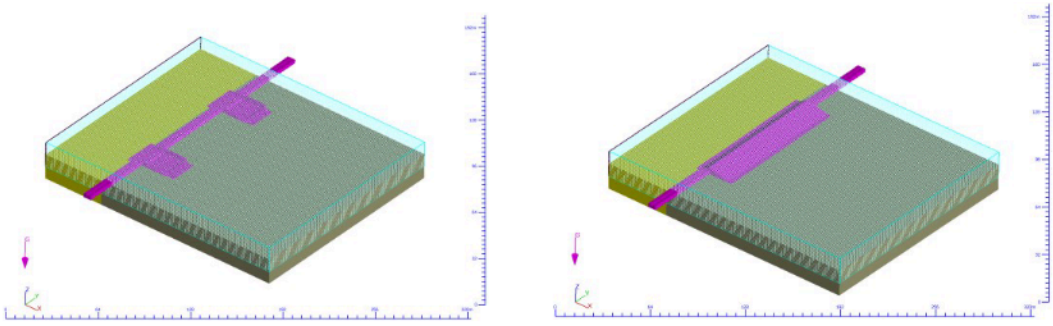

(a) (b)

Figure 14. Meshing setup for both models.

https://doi.org/10.31436/iiumej.v26i3.3825

Table 5. Types and information of the mesh.

Maximum adjacent cell size ratio	Maximum aspect ratio
X direction: 1.00001 < 1.25	X-Y direction: 1.00045 < 3.0
Y direction: 1.00001 < 1.25	Y-Z direction: 1.02263 < 3.0
Z direction: 1.00000 < 1.25	Z-X direction: 1.02308 < 3.0

3. RESULT AND DISCUSSION

3.1. Velocity at Bed

Understanding velocity near the riverbed is important for assessing how sediment erosion occurs downstream of hydraulic structures. In submerged weirs, the bed-level velocity—where water interacts with sediment—greatly influences the size and shape of scour holes. This velocity is affected by weir design, flow rate, and sediment behaviour. High-velocity areas shown in yellow, orange, and red colour contour range indicate strong shear forces that can move sediment and create deeper scour. In contrast, low-velocity areas (shown in blue and green) suggest low-energy zones where sediment tends to settle.

This section compares the velocity patterns at scour depth for two weir types: the adjustable submerged weir (hydraulic tilting gate) and the fixed submerged weir (Crump weir). From the 20 simulations, Run 1 and Run 20 were selected in Table 6 to show how minimum and maximum flow rates impact downstream velocity and scour development. These runs represent a range of flow conditions, from low to extreme, and highlight how different weir designs influence flow behaviour and scouring patterns.

Under low-flow conditions, represented by Run 1 (Q = 183.30 m^3/s), the velocity at the scoured depth reaches up to 1.249 m/s for the Adjustable Submerged Weir, while the Fixed Weir shows a much lower peak of around 0.629 m/s. The velocity contours for both structures are mostly in the blue and green range, indicating low flow energy and a minimal risk of sediment movement. However, the adjustable weir still generates a more concentrated flow jet, suggesting that it may initiate localised erosion even under low discharge conditions, unlike the fixed weir. Under the extreme flow condition of Run 20, the Fixed Weir shows a clear dominance in velocity, reaching 8.978 m/s, while the Adjustable Weir peaks at only 5.152 m/s. The fixed structure generates a highly energetic flow field, with visible signs of turbulence. In contrast, the adjustable weir's jet appears more stable but less intense, possibly due to flow limitations at the gate opening. Overall, the adjustable submerged weir tends to concentrate flow into high-velocity jets, which can cause deeper scour. In contrast, the fixed submerged weir tends to spread the flow energy more broadly, leading to wider and potentially more uniform erosion. These differences highlight how the geometry and design of submerged weirs significantly affect flow behaviour and scour characteristics at the sediment bed.

https://doi.org/10.31436/iiumej.v26i3.3825

Table 6. Comparison of Velocity at Scour Depths Between Original (Adjustable Submerged) Weir and Crump (Fixed Submerged) Weir Across Simulated Flow Run 1 and 20.

Run	Adjustable Submerged Weir (Hydraulic Tilting Gate)	Fixed Submerged Weir (Crump Weir)
1 (Q = 183.30 m^3/s)	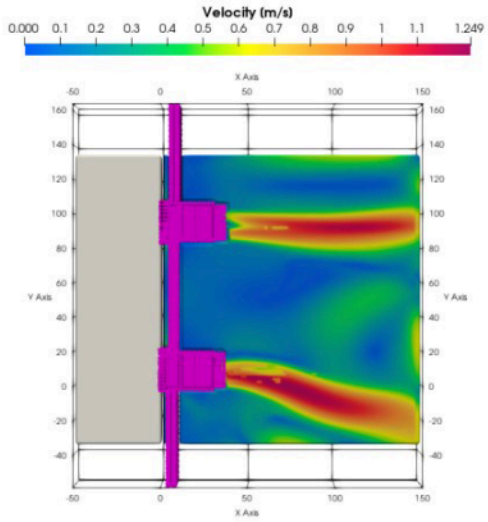 Maximum: 1.249 m/s	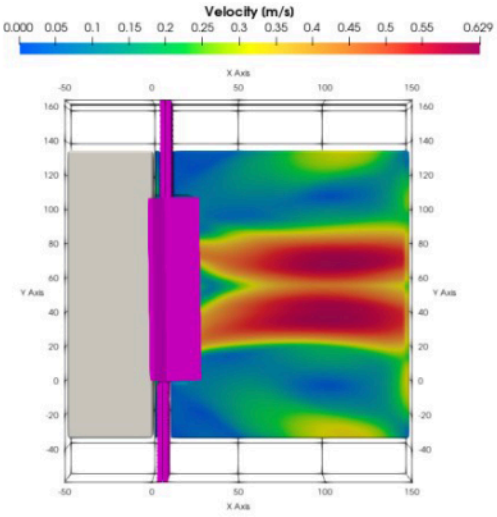 Maximum: 0.629 m/s
20 (Q = 3666.00 m^3/s)	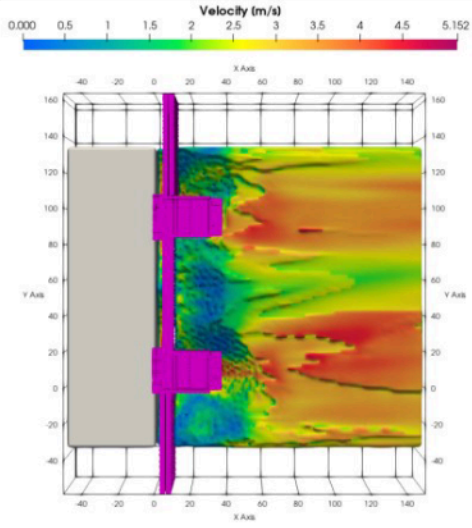 Maximum: 5.152 m/s	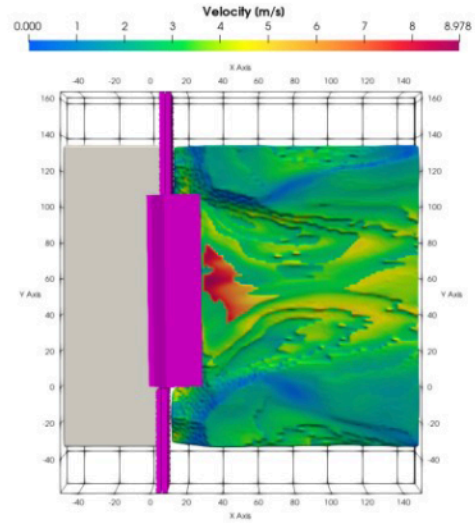 Maximum: 8.978 m/s

The following graph in Figure 15 shows the relationship between velocity at scour depth (V) and discharge (Q) across all 20 simulated runs. On average, the adjustable submerged weir records slightly higher velocity at scour depth, with an average of 4.848 m/s compared to the fixed submerged weir. This trend is supported by the mean values, where the adjustable submerged weir shows 4.590 m/s, while the fixed submerged weir records 4.300 m/s. Although the difference may appear modest numerically, the implications are significant in terms of sediment mobilisation, as velocity increases can result in exponential rises in shear stress and erosion potential.

The maximum velocity for a fixed submerged weir is slightly higher than that of an adjustable submerged weir, with values of 8.978 m/s and 5.152 m/s, respectively. This suggests that under the highest flow conditions, a fixed submerged weir can produce flow intensities equal to or even greater than an adjustable submerged weir. However, the minimum recorded

https://doi.org/10.31436/iiumej.v26i3.3825

velocity is substantially lower for the fixed submerged weir (0.629 m/s) than the adjustable submerged weir (1.249 m/s), indicating more variability and potentially more extensive zones of low-energy flow, which can favour sediment deposition rather than scouring. The velocity at scour depth comparison reveals that an adjustable submerged weir generally produces higher flow velocities during low to medium discharge conditions, which may trigger earlier localised scour. In contrast, at higher discharge levels (after Run 12), the fixed submerged weir begins to match or exceed the adjustable submerged weir in velocity, indicating a shift in hydraulic behaviour. This reflects the fixed submerged weir's tendency to disperse flow energy more broadly, potentially leading to wider yet less concentrated zones. These findings highlight how different weir designs influence the extent of sediment erosion, reinforcing the importance of detailed velocity analysis for effective sediment control.

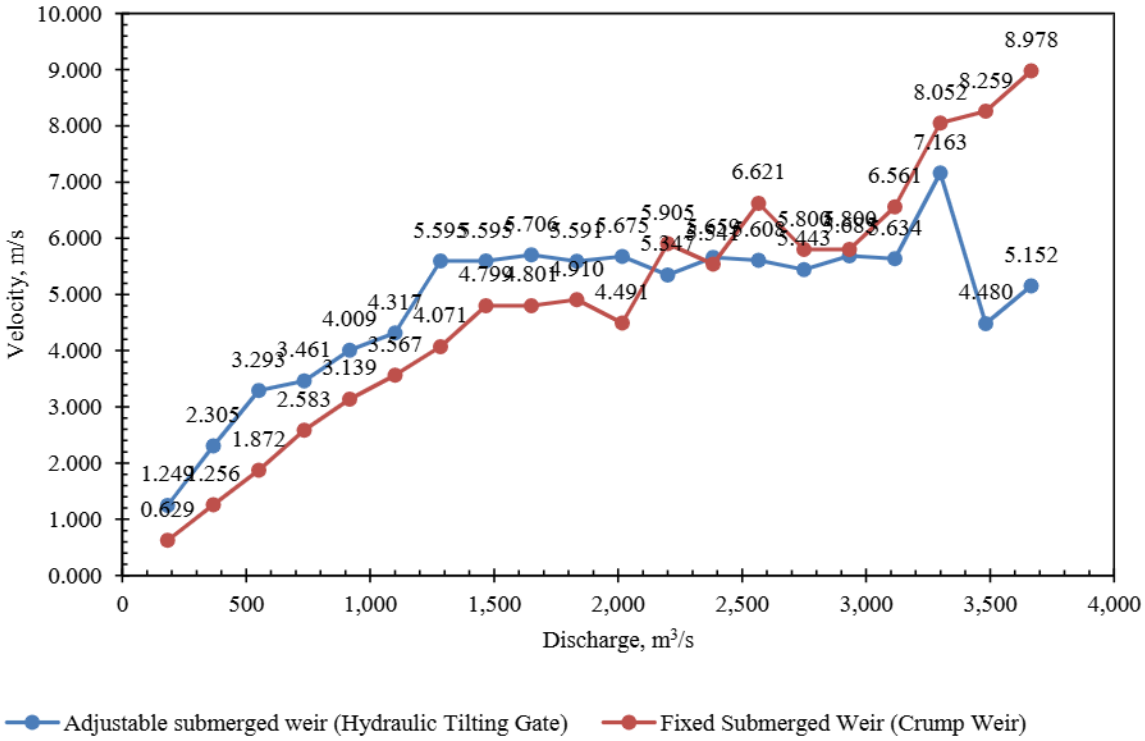

Figure 15. Velocity at Bed (V) versus Discharge (Q) for Adjustable Submerged Weir (Hydraulic Tilting Gate) and Fixed Submerged Weir (Crump Weir).

At higher discharges, the bed velocities downstream of the fixed Crump weir are higher compared to adjustable tilting gates, mainly due to the differences in their shape and flow behaviour. The sloping face of the Crump weir guides higher velocity water directly to the bed, allowing more energy to be transferred and creating stronger forces near the bottom. Conversely, adjustable hydraulic tilting gates produce a jet that is lifted above the bed, and much of its energy is lost through turbulence and recirculation before it reaches the bottom. Tailwater conditions also play a role, as the Crump weir often creates a steeper water-surface slope, which increases flow speed, while gates tend to raise downstream water levels and reduce velocity at the bed. As a result, the Crump weir sustains stronger near-bed velocities, which can influence the extent and pattern of scouring downstream.

3.3. Scour Depth

To study how weir type affects scour development, terrain elevation data from FLOW-3D simulations were analysed for 20 discharge runs, from low to high flow. Each simulation run

https://doi.org/10.31436/iiumej.v26i3.3825

provides a three-dimensional representation of the bed morphology, from which the scour depth is quantified by identifying the difference between the initial and final terrain elevations. The grey area contour plot shows deposition, while the red area contour plot indicates scouring. Table 4 below shows one example of Run 5 at Q = 916.50 m^3/s, comparing the effects of an adjustable submerged weir (Hydraulic Tilting Gate) and a fixed submerged weir (Crump Weir).

For this run, the adjustable submerged weir shows deeper and concentrated scour just downstream of the structure, shown as dark red areas. This is likely due to strong, high-velocity flow jets from the gate. In contrast, the fixed Crump weir results in a wider, more evenly spread erosion pattern, with less depth, suggesting more diffused flow energy. The same analysis method was used for all 20 runs, with constant simulation settings to ensure fair comparison. Overall, the adjustable weir caused stronger and more focused scouring, especially at higher flows, while the fixed weir led to broader but shallower erosion. These results highlight how the design of a weir affects erosion patterns and sediment movement in open channels.

Table 6. Terrain elevation comparison from FLOW-3D for adjustable (Hydraulic Tilting Gate) and fixed (Crump Weir) submerged weirs at Q = 916.50 m^3/s.

Run	Type of weir	Scour Depth
5 (Q = 916.50 m^3/s)	Adjustable Submerged Weir (Hydraulic Tilting Gate)	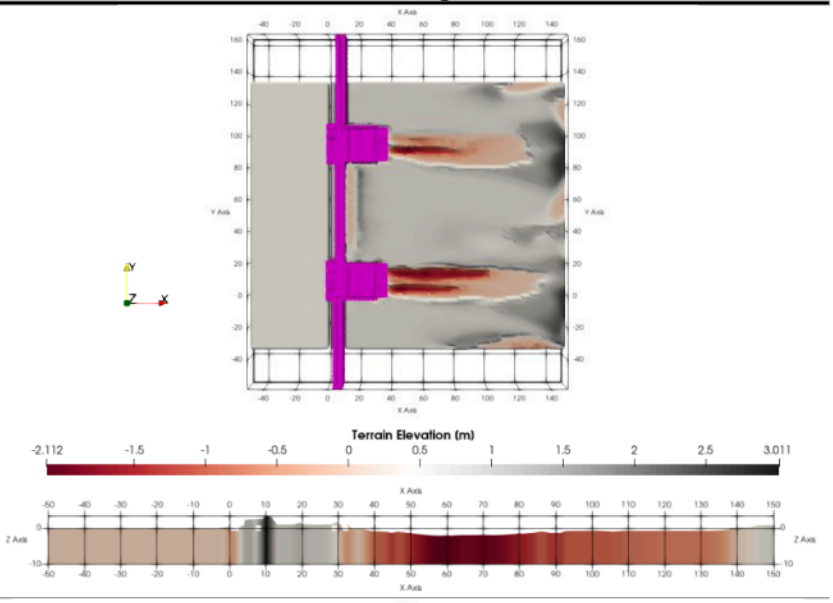
	Fixed Submerged Weir (Crump Weir)	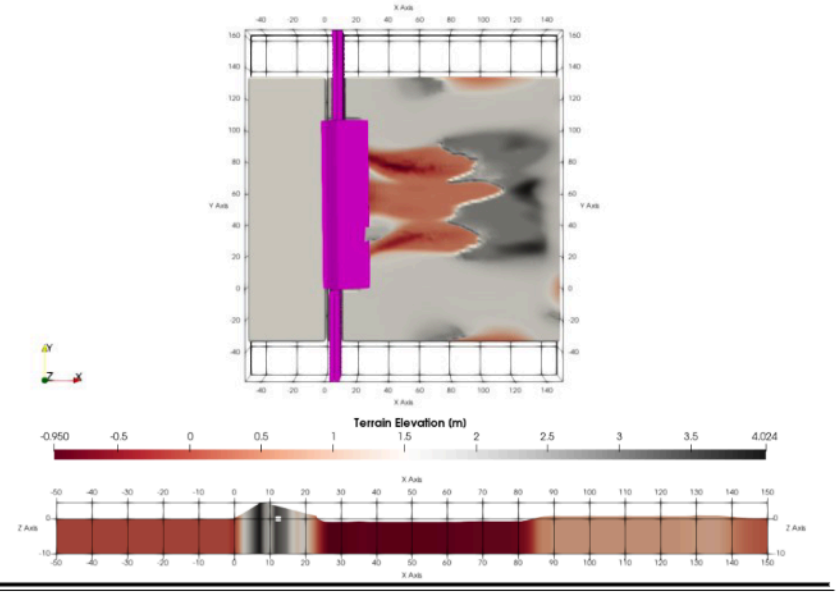

https://doi.org/10.31436/iiumej.v26i3.3825

Figure 16 illustrates the relationship between scour depth (Ds) and discharge (Q) across 20 simulated runs for two types of weirs: an adjustable submerged weir (Hydraulic Tilting Gate) and a fixed submerged weir (Crump weir). Overall, the adjustable submerged weir consistently produces greater scour depth magnitudes, particularly at higher discharge levels. On average, the adjustable weir exhibits a deeper scour magnitude, with a maximum depth of -5.917 m at 3600 m³/s, compared to the fixed weir, which reaches a maximum depth of -5.128 m. This suggests that the hydraulic conditions generated by the adjustable weir are more conducive to intense local erosion, especially as flow increases. The mean scour depth for the adjustable submerged weir is visibly more negative across most discharge levels, indicating more substantial localised erosion. The fixed weir, in contrast, exhibits more moderate and fluctuating scour patterns, particularly in the low to mid-discharge range (up to 1800 m³/s), where its scour depth sometimes remains above -2,000 m. While the fixed submerged weir initially records shallower scour depth at lower flows for runs below 500 m3/s, it begins to narrow the scour depth gap with the adjustable weir as discharge increases beyond 2000 m³/s. This shift could indicate a redistribution of flow energy across a broader area, as fixed weirs like the Crump type are known for diffusing hydraulic intensity more evenly downstream. These results underscore the influence of weir design on sediment transport and bed erosion. The adjustable weir design tends to concentrate flow energy more locally, leading to deeper and more focused scour holes, particularly under extreme flow conditions. Meanwhile, the fixed weir may encourage more distributed erosion patterns, potentially reducing the risk of structural undermining, but increasing the spread of sediment mobilisation zones.

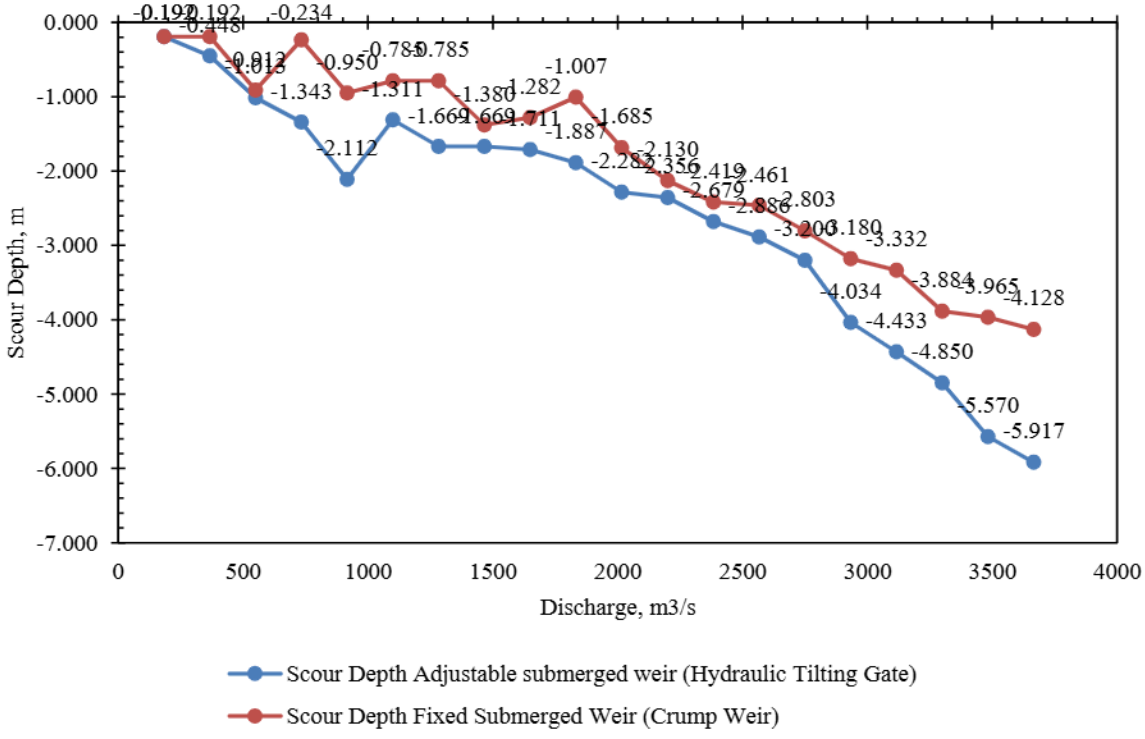

Figure 16. Scour Depth (Ds) versus Discharge (Q) for Adjustable Submerged Weir (Hydraulic Tilting Gate) and Fixed Submerged Weir (Crump Weir)

4. CONCLUSIONS

This numerical investigation using FLOW-3D demonstrates clear differences in sediment scour characteristics downstream of adjustable and fixed submerged weirs under varying flow

conditions. The results show that an adjustable submerged weir (hydraulic tilting gate) tends to produce more concentrated and deeper scouring. In contrast, a fixed submerged weir (Crump weir) generates broader, more distributed erosion patterns. In terms of flow velocity at scour depth, the adjustable weir recorded a higher average velocity of 4.848 m/s, compared to 4.300 m/s for the fixed weir across all simulated runs. The maximum velocity for the adjustable weir peaked at 5.152 m/s. In contrast, the fixed weir reached a higher peak velocity of 8.978 m/s under extreme discharge ($Q = 3666.00\ m^3/s$), indicating its potential for intense flow dispersion and turbulence in high-flow events. Conversely, the minimum recorded velocity was 1.249 m/s for the adjustable weir and 0.629 m/s for the fixed weir, showing that the fixed weir had greater variability and potential for sediment deposition in low-energy zones.

Regarding scour depth, the adjustable weir consistently produced deeper scour holes, with a maximum depth of -5.917 m. compared to -5.128 m for the fixed weir. This pattern was most apparent at higher discharges, suggesting that the concentrated jet flow from the adjustable weir promotes localised erosion. The fixed weir, while showing shallower average scour depths in the early flow stages, begins to approach the scour levels of the adjustable weir as discharge increases beyond 2000 m^3/s, reflecting its broader hydraulic spread.

The findings highlight the importance of weir geometry and operational characteristics in influencing downstream erosion. Adjustable weirs provide hydraulic control but may intensify scour risks, while fixed weirs like the Crump type offer more predictable and distributed sediment transport behaviour, enhancing structural resilience under high-flow conditions. The data derived from this study can support future design improvements and sediment management strategies for submerged weirs in river engineering applications. However, this study is limited to numerical simulations without physical model validation for scouring results, and the scope is confined to clear water scour conditions without sediment supply from upstream. Future research should incorporate experimental validation, investigate sediment-laden flows, and assess the performance of other weir geometries under variable hydraulic and sediment conditions to improve the generalisability and applicability of the findings.

ACKNOWLEDGEMENTS

This study was funded through the IIUM Research Matching Grant Scheme (RMGS) under Project RMGS24-006-0037, titled "Numerical Modelling of Riverbed Scouring Upstream and Downstream of the Kasa Low Weir Structure, Pasir Mas, Across Sungai Kelantan."

REFERENCES

[1] Lo, W. C., Su, H., & Shih, D. S. (2022). Integrating multiple downscaling simulations with continuous in-situ monitoring to assess riverbed scouring. Journal of Hydrology, 610, 127841. https://doi.org/10.1016/j.jhydrol.2022.127841

[2] Bodda, S. S., Gupta, A., Ju, B. S., & Jung, W. Y. (2020). Fragility of a weir structure due to scouring. Computational Engineering and Physical Modeling. https://doi.org/10.22115/cepm.2020.214539.1077

[3] Guan, D., Liu, J., Chiew, Y. M., & Zhou, Y. (2019). Scour evolution downstream of submerged weirs in clear water scour conditions. Water (Switzerland), 11(9). https://doi.org/10.3390/w11091746

[4] Guan, D., Melville, B. W., & Friedrich, H. (2015b). Scour at submerged weirs.

[5] Schleiss, A., De Cesare, G., Franca, M. J., & Pfister, M. (2014). River Flow 2014: Proceedings of the International Conference on Fluvial Hydraulics, Lausanne, Switzerland, 3–5 September 2014. CRC Press/Balkema.

[6] Zhang, W., Liu, X., & Gan, B. (2024). Experimental study on upstream water level rise of submerged rock weirs. Water (Switzerland), 16(15). https://doi.org/10.3390/w16152136

[7] Guan, D., Melville, B. W., & Friedrich, H. (2015a). Live-bed scour at submerged weirs. Journal of Hydraulic Engineering, 141(2). https://doi.org/10.1061/(ASCE)HY.1943-7900.0000954

[8] Guan, D., Melville, B., & Friedrich, H. (2016). Local scour at submerged weirs in sand-bed channels. Journal of Hydraulic Research, 54(2), 172–184. https://doi.org/10.1080/00221686.2015.1132275

[9] Ikinciogullari, E., Emiroglu, M. E., & Aydin, M. C. (2022). Comparison of Scour Properties of Classical and Trapezoidal Labyrinth Weirs. Arabian Journal for Science and Engineering, 47(4), 4023–4040. https://doi.org/10.1007/s13369-021-05832-z

[10] Seyedzadeh, A., Yasi, M., & Farhoudi, J. (2023). Hydraulic characteristics of a sluice gate over a broad-crested weir. Flow Measurement and Instrumentation, 93, 102432. https://doi.org/10.1016/j.flowmeasinst.2023.102432

[11] Seyedzadeh, A., Yasi, M., & Farhoudi, J. (2024). Investigating the flow through parallel sluice gates on a broad-crested weir. Flow Measurement and Instrumentation, 99, 102679. https://doi.org/10.1016/j.flowmeasinst.2024.102679

[12] Moradi, S., Noshahri, A. G., Barati, R., Esmaili, K., & Atashi, V. (2025). Experimental study of Crump weir for sediment transport and flow measurement in sediment-laden rivers. Scientific Reports, 15(1). https://doi.org/10.1038/s41598-025-00404-9

[13] Song, C. G., Park, S. W., & Shin, J. (2024). An experimental study of flow and turbulence properties near the rising sector gate mouth considering the gate opening with a PIV measuring system. Water (Switzerland), 16(20). https://doi.org/10.3390/w16203004

[14] Obaida, A. A. M., & Mohammed, A. Y. (2023). The effect of Crump weir's geometry changes on hydraulic flow characteristics: A review. International Journal of Advanced Natural Sciences and Engineering Researches, 8(8), 47–53. https://as-proceeding.com/index.php/ijanser

[15] Moradi, S., Noshahri, A. G., Barati, R., Esmaili, K., & Atashi, V. (2025). Experimental study of Crump weir for sediment transport and flow measurement in sediment-laden rivers. Scientific Reports, 15(1). https://doi.org/10.1038/s41598-025-00404-9

[16] AL-Naely, H., Al-Khafaj, Z., & Khassaf, S. (2018). Effect of opening holes on the hydraulic performance for Crump weir. International Journal of Engineering, 31(12). https://doi.org/10.5829/ije.2018.31.12c.05

[17] Chen, S. C., & Tfwala, S. S. (2018). Performance assessment of FLOW-3D and X flow in the numerical modelling of fish-bone type fishway hydraulics. In 7th IAHR International Symposium on Hydraulic Structures (ISHS 2018), 272–282. https://doi.org/10.15142/T3HH1J

[18] Jalal, H. K., & Hassan, W. H. (2020). Three-dimensional numerical simulation of local scour around a circular bridge pier using Flow-3D software. IOP Conference Series: Materials Science and Engineering, 745(1). https://doi.org/10.1088/1757-899X/745/1/012150

[19] Sim, Y. C., & Choi, S.-U. (2014). Three-dimensional scour at submarine pipelines under indefinite boundary conditions.

[20] Abd, R. M., & Rady, E.-H. (2011). 2D–3D modeling of flow over sharp-crested weirs. Journal of Applied Sciences Research, 7(12).

[21] Hamad, K., & Torres, C. (2025). Hydraulic analysis with CFD – FLOW-3D numerical modeling of local erosion in bridge piles. Journal of Building Technology, 7(1). https://doi.org/10.32629/jbt.v7i1.3410

[22] Priya Varshini, A. G., Anitha Kumari, K., Janani, D., & Soundariya, S. (2021). Comparative analysis of Machine learning and Deep learning algorithms for Software Effort Estimation. Journal of Physics: Conference Series, 1767(1). https://doi.org/10.1088/1742-6596/1767/1/012019

[23] Chicco, D., Warrens, M. J., & Jurman, G. (2021). The coefficient of determination R-squared is more informative than SMAPE, MAE, MAPE, MSE and RMSE in regression analysis evaluation. PeerJ Computer Science, 7, 1–24. https://doi.org/10.7717/PEERJ-CS.623

[24] Guo, X., Xu, L., Su, L., Deng, Y., & Yang, C. (2021). Comparing Flow Duration Curves and Discharge Hydrographs to Assess Eco-flows. Water Resources Management, 35(14), 4681–4693. https://doi.org/10.1007/s11269-021-02890-8

[25] Aqilah, F., Islam, M., Juretic, F., Guerrero, J., Wood, D., & Ani, F. N. (2018). Study of mesh quality improvement for CFD analysis of an airfoil. IIUM Engineering Journal, 19(2), 203–212. https://doi.org/10.31436/iiumej.v19i2.905

[26] Mojtahedi, A., Soori, N., & Mohammadian, M. (2020). Energy dissipation evaluation for stepped spillway using a fuzzy inference system. SN Applied Sciences, 2(8). https://doi.org/10.1007/s42452-020-03258-0